Cascade Model for Coupled Two-Component Polymer Gels

Ching-Feng Mao, Jia-Chin Chen

Department of Chemical Engineering, Southern Taiwan University of Technology, Tainan, Taiwan, Republic of China

Received 14 April 2005; accepted 15 July 2005
DOI 10.1002/app.22641
Published online 19 December 2005 in Wiley InterScience (www.interscience.wiley.com).

ABSTRACT: A cascade model for the network of coupled two-component polymer gels is presented. The network formation is assumed to be primarily due to the interaction between the functional groups of two unlike polymers. The gel modulus G versus polymer concentration C curve is constructed using the cascade formalism. The variation of G versus C curves with respect to the concentration ratio r of the two components is found to be the characteristics of mixed gels. The model parameters can be obtained by fitting G versus C curves using a nonlinear least-squares method (the gel-modulus approach). The approach is applied to the experimental data for galactomannan/xanthan and glucomannan/xanthan mixed gels. Finally we discuss the gel point predicted by the cascade model. The critical concentration C_0 for the gel point is strongly dependent on r and the functionalities for both polymers. The C_0 versus r curve is easily obtained by experiment, and can be used to evaluate the model parameters (the gel-point approach). The experimental data for galactomannan/xanthan mixed gels is tested to demonstrate the validity of the gel-point approach. The advantages and limitations of both approaches are discussed. © 2005 Wiley Periodicals, Inc. J Appl Polym Sci 99: 2771–2781, 2006

Key words: cascade model; networks; gels; modulus

INTRODUCTION

Polymer gels can be considered as a network consisting of polymer chains interconnected by a number of junction points, with a large amount of solvent enclosed within. According to the mechanism of network formation, polymer gels are grouped in two classes, chemical gels and physical gels. The junction point for a chemical gel is produced via covalent bonding. On the other hand, junction zones are formed in a physical gel due to weakly interacting forces, such as hydrogen bonds, van der Waals forces, and ionic interactions. The elasticity of a polymer gel is due to the tendency of the polymer network to restore its original dimensions when applied forces are removed. Several models have been developed to describe the structure of the polymer network and explore its relation to the gel elasticity.[1–5] The cascade model is currently used as one of the most successful models in analyzing the elastic behavior for a variety of single-component polymeric physical gels.[6,7] However, its ability to model the network for a two-component polymeric physical gel has not been investigated.

A two-component polymer gel is formed when the junctions involve interaction between two structurally different polymers in a solution. This subject finds widespread applications in food industry. For example, galactomannan is often blended with xanthan as additives in a variety of food products to form a mixed gel.[8,9] This synergistic gelation is attributed to the interaction between the galactose-free segment of galactomannan and xanthan.[10,11] Another example is the thermal reversible gelation of starch and hsian-tsao (*Mesona procumbens* Hemsl), a popular dessert in Taiwan and south China. Hsian-tsao polysaccharide is an ionic heteroglycan extracted from hsian-tsao herbs,[12] which becomes a gel in an aqueous solution when heated and cooled in the presence of starch because of the strong interaction between hsian-tsao and starch.[13] Gelation caused by biopolymer mixtures is also an important subject in biological and medical science. For example, actin networks, composed of actin filaments crosslinked by actin-binding proteins (ABPs), play a central role in cell shape maintenance and cell locomotion.[14–16] The elasticity of actin/ABP mixed gels is regulated by the type of ABPs with different crosslinking activities.[16]

The structure of the network for two-component polymer gels has been classified into three categories based on the degree of phase separation and the type of interaction between polymers by Morris:[17]

i. Interpenetrating networks: Two networks are formed separately and interpenetrate each other. No bonds are formed between them, but mutual entanglements may be present.

Correspondence to: C.-F. Mao (cfmao@mail.stut.edu.tw).

ii. Phase separated networks: The incompatibility of the two polymers leads to a phase separated network.
iii. Coupled networks: A gel network is formed due to the intermolecular interaction between the two structurally different polymers.

In this paper, we focus on the coupled network problem and try to establish the cascade formalism for a coupled two-component polymer gel.

In contrast to the rich literature on the experimental works for two-component polymer gels, there are relatively few theoretical works of the network structure of these gels. Pioneering work was reported by Stockmayer,[18] who extended the statistical-mechanical theory of network-forming condensation polymers[19] to two-component condensation polymers and obtained the expressions for the weight-average molecular weight and the gel point. Recently, Tanaka and Ishida[20] combined the lattice theory of polymer solutions developed by Flory[21] and the statistical expressions for condensation polymers to construct the phase diagrams for two-component polymer networks. These phase diagrams demonstrated the sol–gel transition as well as the macroscopic phase separation. After that, Tanaka[22] used the cascade theory to derive the expression for the molecular weight of condensation polymers carrying different species of functional groups, where the limitation of pairwise reaction imposed by Stockmayer was removed. Among these works, no attempt has been made to explain the elastic behavior of two-component polymer gels based on the network structure.

In this paper, the cascade theory for a single-component gel system is extended to model the network for a coupled two-component polymer gel system. The model is then used to predict the elastic modulus–concentration profile and the gel point for a two-component physical gel. Two approaches utilizing a nonlinear curve fitting method are provided to extract the model parameters from experimental data. Examples are given to illustrate the validity of the two approaches.

CASCADE THEORY

The conventional cascade theory for a single-component polymer network is constructed by assuming a pairwise reaction between two functional groups (crosslinking sites) of distinct repeat units

$$\mathrm{A} + \mathrm{A} \leftrightarrow \mathrm{AA} \tag{1}$$

For physical gels, with each polymer chain containing f functionalities (number of functional groups in a polymer chain), the conversion α for the functional groups can be readily determined by the equilibrium relationship

$$K = \frac{\alpha}{(C/M)f(1-\alpha)^2} \tag{2}$$

where K is the equilibrium constant for the reaction, C is the polymer concentration, and M is the molecular weight.

The polymer network is then constructed via the branching process described in the cascade theory,[23] which uses the probability generating function for a binomial process of f trials as roots

$$F_0(\theta) = (1 - \alpha + \alpha\theta)^f \tag{3}$$

where θ is a dummy parameter. Equation (3) can be reasoned as a binomial process with its success probability defined as the conversion of the functional group. The termination of the branching process is characterized by the extinction probability v, which represents the probability of a link becoming extinct (a finite link). The expression for v can be obtained by taking the derivative of eq. (3)

$$v = (1 - \alpha + \alpha v)^{f-1} \tag{4}$$

The physical meaning for eq. (4) is that a link is said to be extinct when the rest of the functional groups are either unreacted $(1-\alpha)$ or reacted but becoming extinct afterward (αv). It is noted that not all the links in a polymer network are elastically effective, but only ties (links leading to infinite branches) are active. The probability generating function for the number of ties in a root $T(\theta)$ is given by replacing α in eq. (3) by $\alpha\,(1-\mathrm{v})$

$$T(\theta) = (1 - \alpha[1 - v] + \alpha[1 - v]\theta)^f \tag{5}$$

The concept of elastically active network chains (EANC) proposed by Scanlan[24] and Case[25] is then used to describe the elasticity of a polymer network. The number of EANCs per repeat unit N_e can be estimated by including only links with more than two ties

$$N_e = \tfrac{1}{2}[T'(1) - T'(0) - T''(0)] \tag{6}$$

The factor one half comes from the fact that the contribution from each tie is counted twice.

We now consider the coupled two-component network system. The network is composed of a mixture of two polymers, each carrying functionalities, f_A and f_B, interacting to form the crosslinking site of the network. A pairwise reaction between functional groups A and B at equilibrium is assumed

$$A + B \leftrightarrow AB \tag{7}$$

It is noted that the conversions of the functional groups, α_A and α_B, must obey the stoichiometric relationship

$$\left(\frac{C_A}{M_A}\right) f_A \alpha_A = \left(\frac{C_B}{M_B}\right) f_B \alpha_B \tag{8}$$

where C_A and C_B, and M_A and M_B are the concentrations and molecular weights of the two polymers, respectively. The equilibrium expression is then written in terms of α_A and α_B

$$K = \frac{\alpha_A}{(C_B/M_B) f_B (1 - \alpha_A)(1 - \alpha_B)} \tag{9}$$

From the combination of eqs. (8) and (9), the values of α_A and α_B can be estimated.

For coupled two-component polymer gels, the network is constructed using two probability generating functions $F_{0A}(\theta)$ and $F_{0B}(\theta)$ in a manner similar to eq. (3)

$$F_{0A}(\theta_A) = (1 - \alpha_A + \alpha_A \theta_A)^{f_A} \tag{10a}$$

$$F_{0B}(\theta_B) = (1 - \alpha_B + \alpha_B \theta_B)^{f_B} \tag{10b}$$

The corresponding extinction probabilities v_A and v_B can be obtained by using the argument that the extinction occurs when the functional groups are either unreacted or reacted but fails to proceed:

$$v_A = (1 - \alpha_A + \alpha_A v_B)^{f_A - 1} \tag{11a}$$

$$v_B = (1 - \alpha_B + \alpha_B v_A)^{f_B - 1} \tag{11b}$$

These two expressions are coupled and the extinction probabilities must be estimated numerically by solving both equations simultaneously. Once the conversions and the extinction probabilities are known, the probability generating functions of the number of ties $T_A(\theta)$ and $T_B(\theta)$ for the two polymers can be obtained according to

$$T_A(\theta_A) = (1 - \alpha_A(1 - v_B) + \alpha_A(1 - v_B)\theta_A)^{f_A} \tag{12a}$$

$$T_B(\theta_B) = (1 - \alpha_B(1 - v_A) + \alpha_B(1 - v_A)\theta_B)^{f_B} \tag{12b}$$

Equation (12) determines the statistical behavior of the numbers of EANCs emanating from the two polymers, N_{eA} and N_{eB}, which are thus expressed in terms of $T_A(\theta)$ and $T_B(\theta)$, respectively, similar to eq. (6)

$$\begin{aligned} N_{eA} &= \tfrac{1}{2}[T'_A(1) - T'_A(0) - T''_A(0)] \\ &= \tfrac{1}{2} f_A \alpha_A (1 - v_B)[1 - v_A - (f_A - 1) \\ &\quad \times \alpha_A v_A (1 - v_B)/(1 - \alpha_A + \alpha_A v_B)] \end{aligned} \tag{13a}$$

$$\begin{aligned} N_{eB} &= \tfrac{1}{2}[T'_B(1) - T'_B(0) - T''_B(0)] \\ &= \tfrac{1}{2} f_B \alpha_B (1 - v_A)[1 - v_B - (f_B - 1) \\ &\quad \times \alpha_B v_B (1 - v_A)/(1 - \alpha_B + \alpha_B v_A)] \end{aligned} \tag{13b}$$

It is evident that the numbers of EANCs in eq. (13) depend on the functionalities, conversions, and extinction probabilities for both polymers. The last two variables are, in turn, determined by the equilibrium constant and the functionalities.

EFFECT OF MODEL PARAMETERS ON THE NUMBER OF ELASTICALLY ACTIVE NETWORK CHAINS

For a single-component polymer gel of a specific polymer concentration, the value of N_e can be readily determined with the knowledge of f and K. For a two-component polymer network, there are two concentrations (C_A and C_B) and two functionalities (f_A and f_B). In the following discussion, we use C to denote the total concentration, r the concentration ratio (C_B/C_A ratio), and s the functionality ratio (f_B/f_A ratio).

We now examine the effects of these model parameters on the normalized N_e (N_e divided by f). All the calculations are performed based on polymer molecular weights of 2×10^6, a typical value for biopolymers. Figure 1 shows the effect of functionality. The curves for both polymers coincide with each other since the concentration ratio and the functionality ratio are taken as unity. Similar to the single-component network system, the value of N_e/f increases with increasing concentration and functionality. Equation (13) suggests that the value of N_e/f is equivalent to half the conversion multiplied by a modifying factor, which is negligible at high concentrations and becomes significant near the gel point ($v = 1$). As a consequence, the increase in N_e/f with increasing concentration is somewhat parallel to that of conversion above the gel point. Below the gel point, the extinction probability becomes unity and all the network branches are finite, thus leading to an N_e value of zero.

The effect of equilibrium constant on N_e/f is illustrated in Figure 2. The conversion and the number of EANCs increase with increasing equilibrium constant. The increasing trend with respect to concentration in

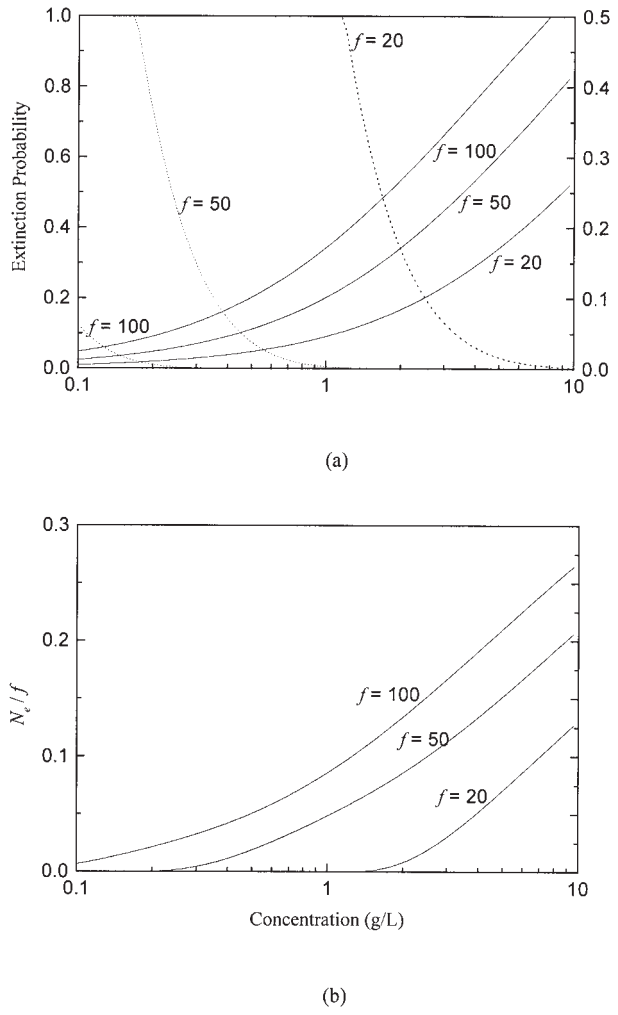

Figure 1 Conversion, extinction probability, and N_e/f as a function of concentration at different functionalities with $r = 1$, $s = 1$, and $K = 10^4$ L/mol. (a) Solid curves: conversion; dotted curves: extinction probability; (b) N_e/f.

Figure 2 is similar to that in Figure 1. It is noted that the extinction probability for the K value of 10^6 L/mol is so small that it cannot be seen in the graph.

The effects of s and r are quite different from those of f and K. The deviation of these ratios from unity causes a splitting of the curve in two. Figure 3 shows the effect of the variation of s at a fixed f_A. It can be seen that N_{eA}/f_A increases with increasing functionality ratio because of the increase in f_B when the value of f_A is fixed. On the other hand, the curves for N_{eB}/f_B are much lower than those for N_{eA}/f_A, and the larger the s value, the larger the difference will occur. This difference is due to the shortage of functional groups A to react with functional groups B at high s values. It is noted that the extinction probability curves for A and B almost overlap with each other and the curves shift towards low concentration region at high s values. The reduction in extinction probability at high s values leads to a decrease in gel point, thus allowing the presence of elastically active network chains at low concentrations. The functionality ratio below unity is not examined here since the polymer with function group A is arbitrarily set as the polymer having the lowest functionality.

Figure 4 demonstrates the effect of concentration ratio on the gel network. It can be seen that α_A increases with increasing concentration ratio because of an increase in the amount of functional groups B. However, the change of N_{eA} does not follow the same trend since v_A and v_B may become higher at high concentration ratios. The increase in v and gel point at high r values is simply due to the fact that the change of v_A is coupled with v_B, which increases significantly when the concentration for functional groups A becomes lower, thus leading to an increase in v_A. Figure 4 also shows that the value of N_{eB}/f_B is progressively lower than that of N_{eA}/f_A at higher r values. The curves for $r < 1$ are not shown because they overlap

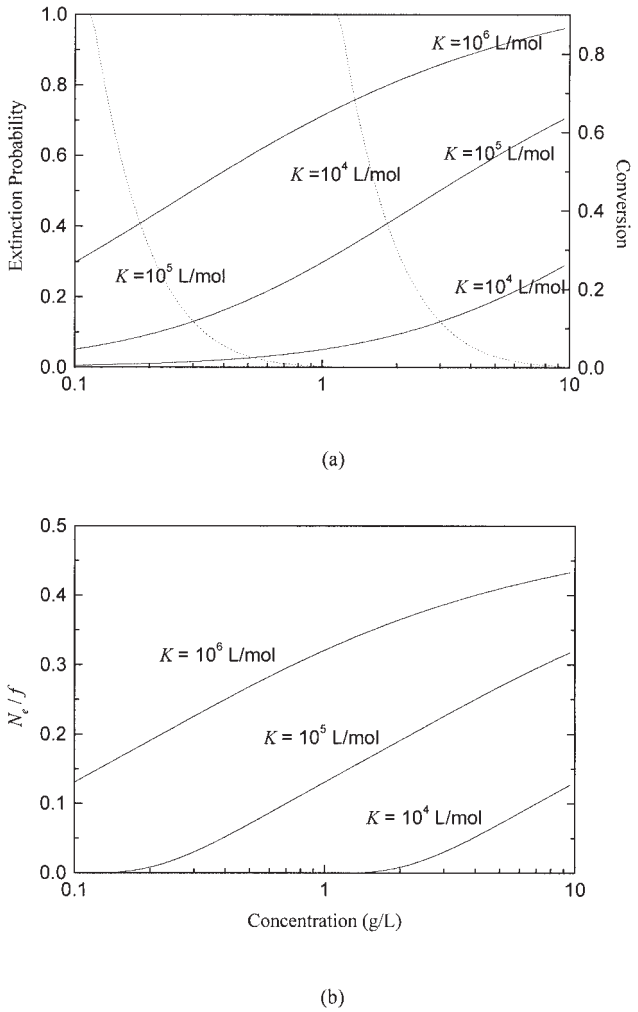

Figure 2 Conversion, extinction probability, and N_e/f as a function of concentration at different equilibrium constants with $r = 1$, $s = 1$, and $f = 20$. (a) Solid curves: conversion; dotted curves: extinction probability; (b) N_e/f.

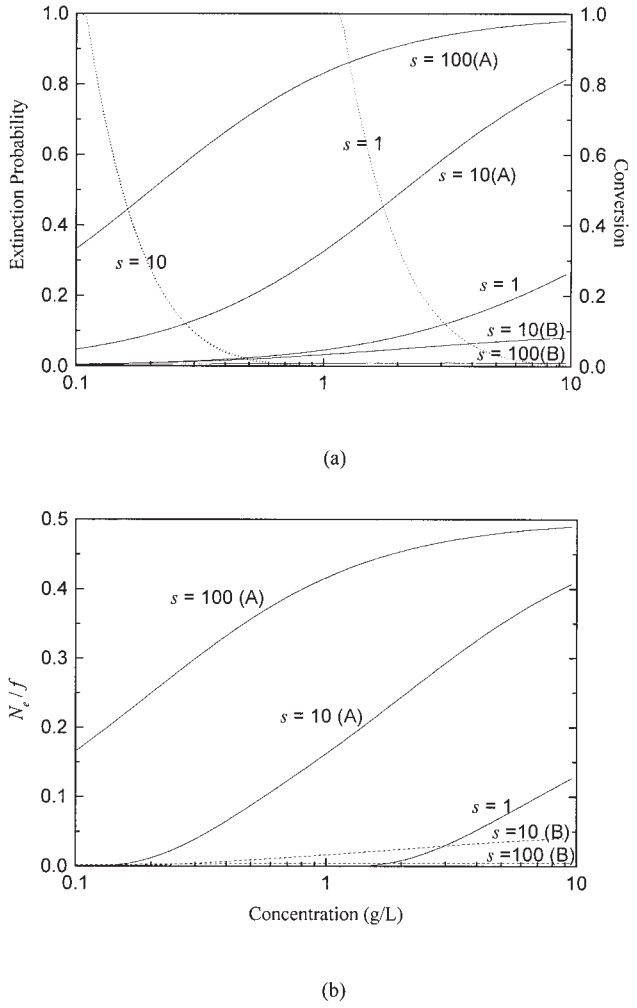

Figure 3 Conversion, extinction probability, and N_e/f as a function of concentration at different functionality ratios with $r = 1$, $f_A = 20$, and $K = 10^4$ L/mol. (a) Solid curves: conversion; dotted curves: extinction probability; (b) Solid curves: N_{eA}/f_A; dotted curves: N_{eB}/f_B.

with those with $r > 1$. For example, the curves for $r = 0.1$ are identical to those for $r = 10$ but the labels for A and B are switched. This symmetry fails when the value of s is different from unity.

ELASTICITY OF GELS

Clark and Ross-Murphy have proposed that the gel modulus of a polymer gel can be approximated by the elastic expression for a rubber[7]:

$$G = aRTN_e(C/M) \qquad (14)$$

where RT denotes the entropy gain per mole of active network chains during a relaxation process and a is the front factor, reflecting deviations from ideal rubber elasticity. For a coupled two-component polymer gel, eq. (14) is rewritten by combining the contributions from polymers A and B

$$G = aRT[N_{eA}(C_A/M_A) + N_{eB}(C_B/M_B)] \qquad (15)$$

The modulus for a specific concentration can be calculated using eq. (15) if other parameters are known. In contrast to the single-component polymer gel, two more parameters, r and f_B (or s), in addition to a, K, and f_A, are required to evaluate the gel modulus. Practically, r is the parameter that can be adjusted by the experimentalists while s is essentially the material property of the system. In the following we will investigate the effects of these parameters on the elastic behavior of gels. The result will provide a guideline for making a first approximation of the model parameters from experimental data.

The gel modulus simply increases with increasing a, K, or f, exactly like the behavior for a single-compo-

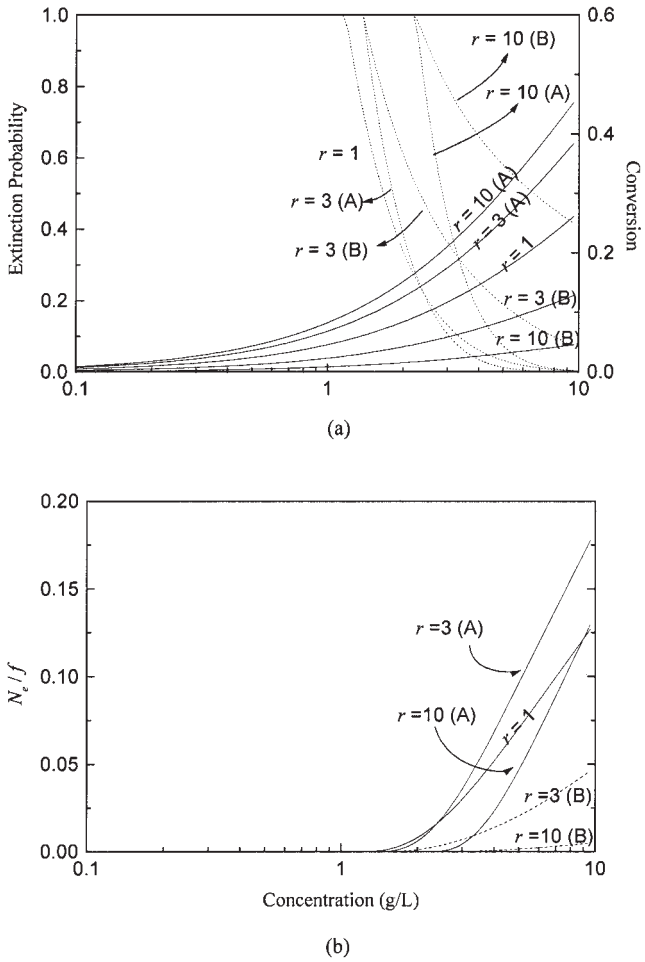

Figure 4 Conversion, extinction probability, and N_e/f as a function of concentration at different concentration ratios with $s = 1$, $f_A = 20$, and $K = 10^4$ L/mol. (a) Solid curves: conversion; dotted curves: extinction probability; (b) Solid curves: N_{eA}/f_A; dotted curves: N_{eB}/f_B.

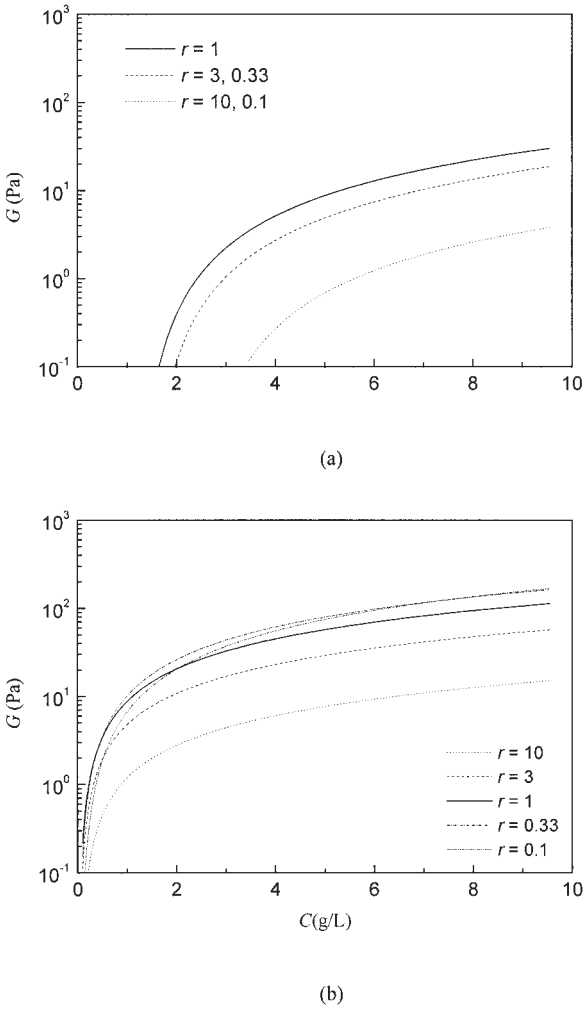

Figure 5 Concentration dependence of G at different concentration ratios with $a = 1$, $f_A = 20$, and $K = 10^4$ L/mol. (a) $s = 1$; (b) $s = 50$.

nent polymer gel. Therefore the effects of these parameters are not examined here. Here, we focus on the effects of r and s. Figure 5 illustrates the G versus C curves at different values of r and s. The curves are obtained by arbitrarily setting the temperature to be 298 K and the molecular weights for both polymers to be 2×10^6. When the functionalities for both polymers are identical [Fig. 5(a)], the gel modulus decreases as the extent of the deviation of concentration ratios from unity becomes larger, thus having the largest value at $r = 1$ for a specific polymer concentration. It can be seen that the G versus C curves with reciprocal r values overlap each other. For the gel systems with the functionality ratios other than unity [Fig. 5(b)], the largest values of moduli may not occur at $r = 1$ and the G versus C curves with reciprocal r values do not overlap. At high s values, the G versus C curves with $r < 1$ lies higher than those with $r > 1$, and vice versa. This result suggests that the experimental G versus C curves at different r values can be used to judge which polymer contains more crosslinking sites. It also implies that simultaneously using the G versus C curves at several r values is required to ensure a proper estimation of f_A and f_B on extracting the model parameters from experimental data.

Since the modulus–concentration data can be obtained directly from experiments, a computer code capable of curve fitting these data using eq. (15) was developed. This method is named the gel-modulus approach in this article. The program code was written employing the Levenberg–Marquardt (nonlinear least-squares optimization) algorithm,[26] and allowing data at various r values to be fitted simultaneously. The best fit is obtained by minimizing the object function

$$\chi^2 = \sum (G_i^{\exp} - G_i^{\mathrm{mod}})^2 \tag{16}$$

It is noted that the parameters a and K are estimated by the Levenberg–Marquardt algorithm while the best-fit values of f_A and f_B to be found using a direct search method because of their discrete nature.

Next we demonstrate the gel-modulus approach to extracting the model parameters from modulus–concentration data. Unlike single-component polymer gels, very few experimental modulus–concentration data can be found in the literature. Goycoolea et al.[27] have examined the synergistic gelation of xanthan gum (XG) with locust bean gum (LBG) or konjac mannan (KM). They proposed that the binding site involves the interaction of one segment of LBG or KM with one segment of XG. This feature ensures that their data can be used to demonstrate the elastic behavior of coupled two-component polymer gels.

Figure 6 shows the variation of gel modulus at

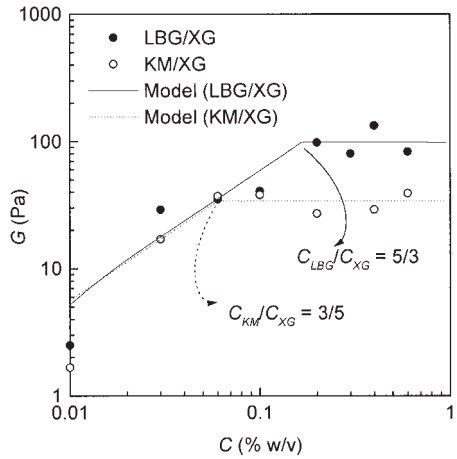

Figure 6 Testing of the elastic model using eq. (15) for two-component gels of 0.1% (w/v) deacetylated xanthan mixing with locust bean gum (LBG) or konjac glucomannan (KM) (data from Goycoolea et al.[27]). The concentration on the abscissa refers to LBG (●) or KM (○).

different concentrations of LBG or KM for the LBG/XG or KM/XG mixed gels at 283 K, reported by Goycoolea et al.[27] It is noted that this figure is different from Figure 5 by that the concentration of XG is fixed at 0.1% (w/v) while that of LBG or KM, rather than the total concentration, is allowed to change. It can be seen that the gel modulus increases steadily with increasing LBG or KM concentration, and then levels off at high LBG or KM concentrations. Xanthan is known to form a weak gel in aqueous solutions. Here we assume that the elasticity of xanthan weak gel has a minor contribution to the overall gel modulus and can be neglected from the model. The extremely low values of gel moduli at low C_{LBG}/C_{XG} or C_{KM}/C_{XG} confirm this assumption.

The molecular weight of each polymer was not reported in the original paper. Here we assume their molecular weights to be approximately 10^6 in all cases, which is considered to be reasonable for these polysaccharides. Once all the variables—temperature, ingredient concentrations, molecular weights—required by the computer program are known, the data are ready to be tested with the cascade equation.

The optimized value of the object function was obtained at numerous set of f_A and f_B, and the results are plotted in Figure 7. It is noted that several local minima appear for both mixed gels. The uncertainty is due to the scarcity of data points. This problem can be eliminated if the G versus C curves were obtained at different r values like Figure 5.

In Figure 7(a), the object function has the lowest value when $f_{LBG} = 30$ and $f_{XG} = 50$. To verify the validity of these figures, the chemical structure of these polymers has to be considered. The primary structure of LBG consists of a backbone of mannan with randomly attached single galactose side chains.[28] It has been proposed that the intermolecular association between LBG and other polysaccharides occurs in the region with more than six consecutive galactose-free mannose residues.[29] In view of the theoretical prediction of the distribution of galactose-free mannan blocks,[30] a value of 30 for f_{LBG} is somewhat lower than the theoretical value. On the other hand, the primary structure of xanthan gum is constructed via repeating units composed of five monosaccharide residues. A value of 50 for f_{XG} implies that a junction zone is formed in approximately every 20 repeating units along the XG backbone. Therefore, both of the best-fit values for f_{LBG} and f_{XG} are consistent with their chemical structures.

For the KM/XG mixed gel, the object function has the lowest value when $f_{KM} = 500$ and $f_{XG} = 300$ [Fig. 7(b)]. The f_{XG} value is too high since it corresponds to a junction zone occurring in every three repeating units. The only reasonable functionality set in Figure 7(b) is the functionality set with $f_{KM} = 50$ and $f_{XG} = 30$. The validity of the f_{KM} value can be reasoned as follows: Konjac mannan is a glucomannan consisting of mannose and glucose residues in a ratio of approximately 2 : 1, with a low degree of acetyl substituents (~6%).[31] Gelation can be induced after deacetylation by alkali treatment,[32] indicating that the crosslinking is formed via unsubstituted glucomannan backbone. It has also been reported that the interaction of konjac mannan with cellulose can be attributed to its unsubstituted mannan segments.[33] Since the unsubstituted mannan content in konjac mannan is higher than that in LBG, it is reasonable to have f_{KM} greater than f_{LBG}.

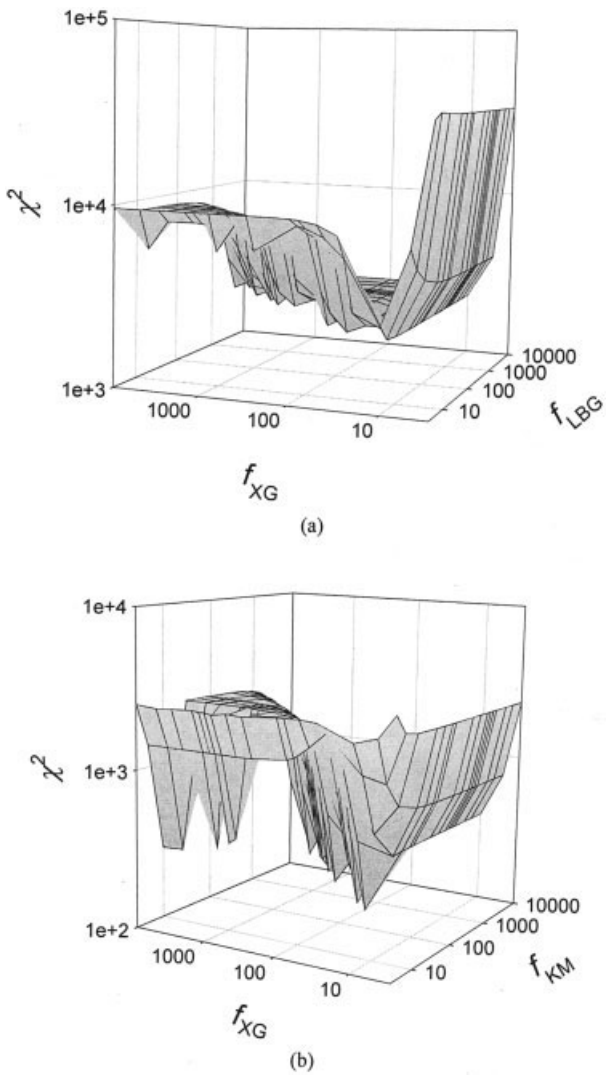

Figure 7 The object function χ^2 as a function of functionalities obtained by fitting the data of Figure 6 using eq. (15). (a) LBG/XG mixed gels; (b) KM/XG mixed gels.

The fitting parameters of the cascade equation are listed in Table I. The front factors a in both cases are close to unity, a typical value for rubbers, indicating the entropic nature of the gel elasticity. This result also suggests that the flexibility of the network strands for LBG/XG or KM/XG mixed gels is similar to that of ideal rubbers. This behavior seems to be in contradic-

TABLE I
Fitting Results for the Modulus–Concentration Data in Figure 6, using Eq. (15)

	f_{LBG}	f_{KM}	f_{XG}	a	K (L/mol)	χ^2 (Pa^2)
LBG/XG gels	30	–	50	0.84	7.6×10^{10}	2060
KM/XG gels	–	50	30	0.48	2.1×10^{8}	148
KM/XG gels	–	500	300	0.048	1.3×10^{19}	139

tion to the stiffness of the helix structure of XG. A possible explanation is that the segment of XG between junction zones does not adopt a helical conformation, but rather a flexible conformation. It is also possible that the attachment of mannan occurs on the disordered segments of xanthan, as suggested by Goycoolea et al.[27] The value of 50 or 30 for f_{XG} in the LBG/XG or the KM/XG system is consistent with this model. In case of $f_{KM} = 500$ and $f_{XG} = 300$, the parameter a is even lower and unrealistic. It is also noted that the equilibrium constants K for both mixed gels are enormously high, reflecting that the heterogeneous binding of XG with LBG or KM is a preferred reaction.

The G versus C curves generated by using the fitting parameters in Table I generally agree with the experimental data, as shown in Figure 6. The starting point of the constant-modulus plateau of these curves can be clearly identified at 1.67 and 0.60 for C_{LBG}/C_{XG} and C_{KM}/C_{XG}, respectively. These points correspond to the concentration ratios that satisfy the stoichiometric equivalence

$$\frac{C_{LBG}f_{LBG}}{M_{LBG}} = \frac{C_{XG}f_{XG}}{M_{XG}} \text{ or } \frac{C_{KM}f_{KM}}{M_{KM}} = \frac{C_{XG}f_{XG}}{M_{XG}} \qquad (17)$$

The conversions for both polymers approach a value of unity at these points simply because of the high K values. With C_{XG} fixed, below the stoichiometric equivalence point, f_{LBG} or f_{KM} is almost completely consumed, whereas, in the plateau regime (above the stoichiometric equivalence point), f_{XG} is almost completely reacted.

The model parameters obtained from Figure 6 can be used to explain the composition dependence of the enthalpy of gelation reported by Goycoolea et al.,[27] where, with C_{XG} fixed, the enthalpy of gelation steadily increases with increasing C_{KM} until it reaches a constant value at high C_{KM} (Fig. 8). The enthalpy data were reported per gram of XG in ref. 27 and they were replotted after normalized by ΔH_{max}, the average ΔH values at high C_{KM}. By assuming that all the crosslinking sites are identical and the enthalpy of reaction is not affected by the reacted functionalities, the conversion of XG can thus be approximated by the normalized enthalpy of gelation. It can be seen that the curve generated by using the cascade parameters in Table I agrees fairly with the normalized data. It is noted the lowest C_{KM} in Figure 8 to achieve ΔH_{max} ($C_{KM}/C_{XG} \sim 1$) is somewhat higher than that to achieve G_{max} in Figure 6. This difference may be due to the complexity of the binding reaction for the KM/XG gel. However, the cascade formalism given in this article is developed based on a simple reaction scheme, which predicts the starting point of the constant–enthalpy plateau occurring at $C_{KM}/C_{XG} = 0.6$.

GEL POINTS PREDICTED BY THE CASCADE THEORY

For a polymer gel system, the gel formation requires a minimum polymer concentration, which is called the gel point. The gel point is the concentration in Figures 1–4, where $v = 1$ or in Figure 5 where G approaches zero. The cascade formalism for polymer gel networks provides a simple approach to estimating the gel point: Below the gel point (i.e., the sol state), the extinction probability is always unity, while, above the gel point (i.e., the gel state), the extinction probability has a value less than unity. This fact indicates that a critical condition will be encountered when solving eqs. 4 or 11 at the sol–gel transition. For a single-component polymer gel, the critical condition can be readily obtained by finding the minimum of the function of eq. (4)

$$\Psi = (1 - \alpha + \alpha v)^{f-1} - v \qquad (18)$$

at the sol–gel transition, namely, calculating the critical conversion α_0, which satisfies the following derivative

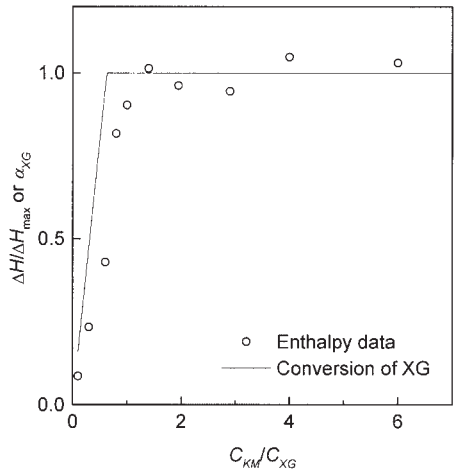

Figure 8 Composition dependence of the enthalpy of gelation for KM/XG mixed gels (data from Goycoolea et al.,[27] only data set with $C_{XG} = 0.1\%$ (w/v) was used). The solid curve represents the composition dependence of the conversion of XG predicted by the cascade parameters in Table I.

$$\frac{d\Psi}{dv}(v = 1) = 0 \tag{19}$$

The solution of eq. (19) leads to the classical Flory's result[34]

$$\alpha_0 = \frac{1}{f - 1} \tag{20}$$

In a similar way the critical conversions for a coupled two-component polymer gel can be obtained by evaluating the derivative of eq. (11) at $v = 1$

$$\alpha_{A0} = \left[rs\left(\frac{M_A}{M_B}\right) \right]^{1/2} ((f_A - 1)(f_B - 1))^{-1/2} \tag{21a}$$

$$\alpha_{B0} = \left[rs\left(\frac{M_A}{M_B}\right) \right]^{-1/2} ((f_A - 1)(f_B - 1))^{-1/2} \tag{21b}$$

By combining a_{A0} and a_{B0}, we find that eq. (21) is reduced to the Stockmayer's gelation condition[18]

$$\alpha_{A0}\alpha_{B0} = 1/(f_A - 1)(f_B - 1) \tag{22}$$

The critical concentration (the sum of C_A and C_B) at the gel point can then be calculated by substituting eq. (21) into the equilibrium expression [eq. (9)]:

$$C_0 = \frac{(1 + r)\alpha_{A0}M_B}{rKf_B(1 - \alpha_{A0})(1 - \alpha_{B0})} \tag{23}$$

Equations (21) and (23) indicates that C_0 is a function of r, K, f_A and f_B, and M_A and M_B. Among these parameters, M_A and M_B are determined experimentally, while r can be adjusted by experimentalists to produce mixed gels with different C_0.

A mixed gel can be characterized by the composition dependence of C_0, which is determined by K, f_A and f_B. Equation (23) shows that C_0 is simply inversely proportional to K, whereas the effect of f_A and f_B is somewhat complicated. Figure 9 illustrates the effect of f_A and f_B on the composition dependence of C_0. The polymer molecular weights and the equilibrium constant are arbitrarily set to be 2×10^6 and 10^4 L/mol, respectively. The critical concentration is normalized according to the C_0 value at $r = 1$ for each curve to compare them in the same plot. It can be seen that when $f_A = f_B$ [Fig. 9(a)], C_0 has a minimum at $r = 1$ and increases symmetrically away from the $r = 1$ axis. The normalized C_0 versus r curve shifts downward with increasing functionality. The result is similar to that predicted by Figure 4, which shows that the critical point (the concentration where v becomes unity) has a minimum at $r = 1$. At higher functionality ratios [Fig. 9(b)], the C_0 versus r curves behave somewhat different. The minimum value of C_0 shifts leftward and the curves of different functionalities almost overlap each other in the left half, such that the symmetry no longer exists.

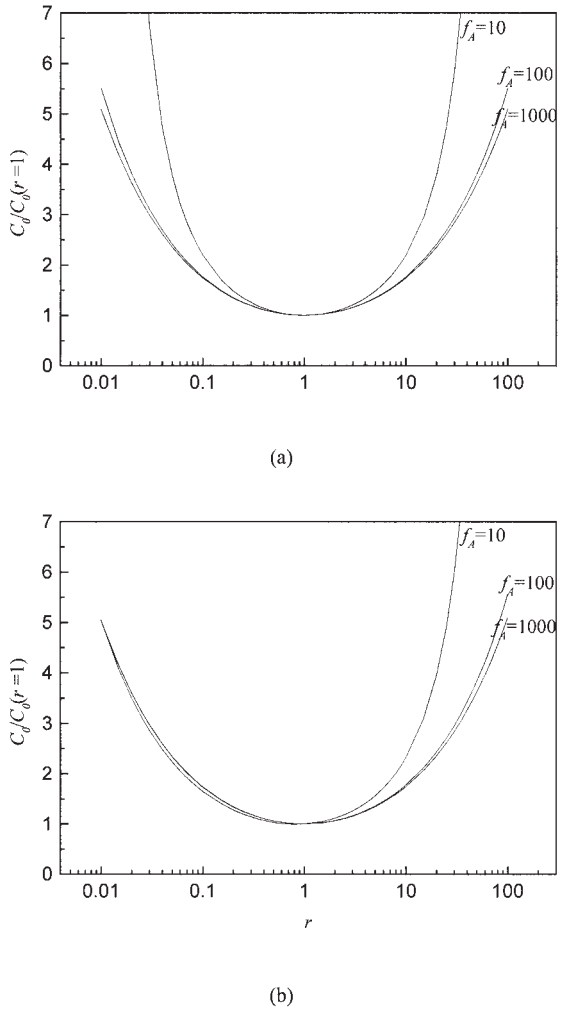

Figure 9 Composition dependence of the critical concentration at different functionalities for polymer A with $K = 10^4$ L/mol. (a) $s = 1$; (b) $s = 10$.

The difference in Figure 9(a,b) shows that the C_0 versus r curve strongly depends on the functionality ratio. Figure 10 demonstrates the normalized C_0 versus r curves at different s values. When $f_B > f_A$ (s greater than unity), the left part of the curve becomes lower and the minimum value of C_0 shifts leftward, indicating that the formation of gel networks is favored in the region where $C_B < C_A$; when $f_B < f_A$ (s less than unity), the whole curve shift to the right, indicating that the formation of gel networks is favored in the region where $C_B > C_A$. The strong dependence of C_0 versus r curves on f_A and f_B suggests that they can be used to estimate the parameters of the cascade model. The advantages of using C_0 versus r curves rather than G versus C curves are that the empirical factor a does not appear in eq. (23) and the C_0 versus r curve can be

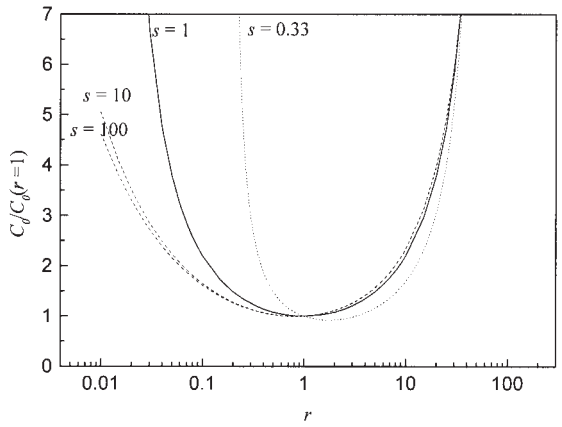

Figure 10 Composition dependence of the critical concentration at different functionality ratios with $f_A = 10$ and $K = 10^4$ L/mol.

measured using a relatively inexpensive experimental setup. This method is named the gel-point approach in this article.

In the following, LBG/XG mixed gels are re-examined to demonstrate the gel-point approach. The mixed gel was prepared via mixing LBG (Sigma, St. Louis, MO) with a mannose/galactose ratio of 3.28 (determined by the alditol acetate method[35]) and XG (Aldrich, Milwaukee, MI) at room temperature in de-ionized water and then heating to 85°C for 30 min. The molecular weights of LBG and XG, estimated using the Mark-Houwink equation,[36,37] are 1.69×10^6 and 9.80×10^5, respectively. The critical concentration was determined with a series of mixed gels of different concentrations by the "test tube upside-down" method.[38]

Figure 11 shows the experimental C_0 versus r data for the LBG/XG mixed gel, where r is defined as C_{LBG}/C_{XG}. At first glance, the composition dependence of C_0 suggests a large f_{LBG} along with a small f_{XG}, similar to the curves with high s values in Figure 10. Since xanthan is known to form a weak gel in aqueous solution,[39] we examined its effect on C_0 by measuring pure xanthan solutions using the "test tube upside-down" method, which results in a C_0 value identical to that at $r = 0.01$. This result indicates that the gel network at the lowest r value is mainly due to the self-association of xanthan, which is against the nonself-association assumption in our model.

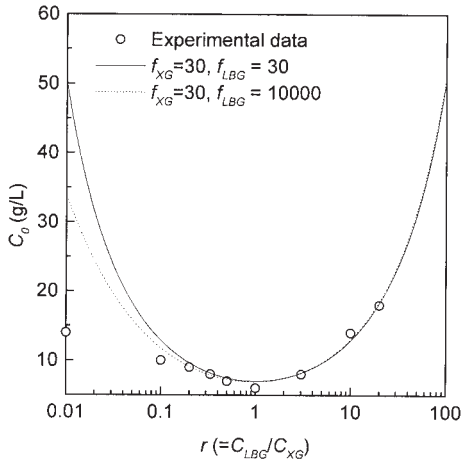

Figure 11 Composition dependence of the critical concentration for LBG/XG mixed gels at 313 K (r defined as C_{LBG}/C_{XG}).

It is evident that, in the C_0 measurement, significant deviation from the ideal coupled network occurs at low r values, consequently leading to an erroneously high f_{LBG} value. In the measurement of gel modulus, the weak gel behavior does not interfere the measurement since the network of weak gels breaks up under a shear stress. Therefore, effort has been made to bypass this problem by utilizing the data with $r > 0.3$ to fit eq. (23).

Some of the best-fit parameters obtained by using the data with $r > 0.3$ are listed in Table II. The object function in Table II is defined as the summation of the square of the difference between the observed and the calculated C_0 values

$$\chi^2 = \sum (C_{0i}^{\text{exp}} - C_{0i}^{\text{mod}})^2 \tag{24}$$

It can be seen that the best-fit value for f_{XG} is always 30, which is comparable to that obtained from the modulus–concentration data. On the other hand, the best-fit value for f_{LBG} ranges from 30 to 10,000, or even higher. Among them, the highest value gives the lowest χ^2; however, this f_{LBG} value is too high to be realistic. If we compare the curves for $f_{LBG} = 30$ and 10,000 with the experimental data (shown in Fig. 11), it turns out that both curves fit the data very well. The uncertainty for the determination of f_{LBG} is due to the partial usage of the data in the left half and the minor contribution of XG self-association to the fitted data, which becomes worse at lower temperatures. Consequently, it is concluded that the f_{LBG} value cannot be determined without ambiguity for LBG/XG mixed gels by using the gel-point approach.

TABLE II
Best-Fit Results for the Critical Concentration–Concentration Ratio Data in Figure 11, using Eq. (23)

f_{LBG}	f_{XG}	K (L/mol)	χ^2 (g^2/L^2)
30	30	450	3.54
50	30	260	2.97
100	30	130	2.64
1000	30	13	2.41
10,000	30	1.3	2.40

CONCLUSIONS

We have extended the cascade theory for single-component polymer gels to describe the network for coupled two-component polymer gels. The interaction between the two components is assumed to follow a pairwise reaction at equilibrium. The cascade network is then developed using the probability generating function for each repeating unit based on the branching theory. The probability generating function is a function of the conversions and extinction probabilities for both components, which are in turn determined by the equilibrium constant and the functionalities for both components. Finally, we present the expressions for the gel modulus and the gel point derived from the cascade formalism.

The parameters of the cascade model for a specific mixed gel system can be extracted from the experimental data using a nonlinear curve fitting method. In this article, we provide two approaches to estimating these parameters: the gel-modulus approach and the gel-point approach. The former involves using the G versus C curves at different concentration ratios, while the latter utilizes the C_0 versus r curve at the critical condition. We have demonstrated that both approaches could be applied to the analysis of galactomannan/xanthan or glucomannan/xanthan mixed gels. However, special care must be taken in interpreting the result.

The abnormal behavior shown in the composition dependence of C_0 for galactomannan/xanthan mixed gels reminds us that the gelation of two-component polymer system is often a complicated process. The model proposed in this paper is limited to the system where the network is formed via the interaction between unlike polymers (coupled network). Despite the complexity in most mixed gels, we hope that this model can be used to explain or predict the elastic behavior and the critical condition for the gel systems caused by synergistic interaction between two structurally different polymers. Investigation of the fitting parameters can also shed some light on the nature of the junction zones of these gels. Moreover, for future research, our model serves as a starting point from which specific models can be developed to describe the network of mixed gels formed via other interaction patterns.

References

1. Ross-Murphy, S. B.; McEvoy, H. Br Polym J 1986, 18, 2.
2. Clark, A. H.; Ross-Murphy, S. B. Adv Polym Sci 1987, 83, 57.
3. Watase, M.; Nishinari, K.; Clark, A. H.; Ross-Murphy, S. B. Macromolecules 1989, 22, 1196.
4. Jones, J. L.; Marques, C. M. J Phys Fr 1990, 51, 1113.
5. Stauffer, D.; Coniglio, A.; Adam, M. Adv Polym Sci 1982, 44, 103.
6. López, D.; Mijangos, C.; Muñoz, M. E.; Santamaría, A. Macromolecules 1996, 29, 7108.
7. Clark, A. H.; Ross-Murphy, S. B. Br Polym J 1985, 17, 164.
8. Imeson, A. Thickening and Gelling Agents for Food; Kluwer: London, 1996.
9. Dea, I. C. M.; Morris, E. R.; Rees, D. A.; Welsh, E. J.; Barnes, H. A.; Price, J. Carbohydr Res 1977, 57, 249.
10. McCleary, B. V.; Dea, I. C. M.; Windust, J.; Cooke, D. Carbohydr Polym 1984, 4, 253.
11. Pai, V. B.; Srinivasarao, M.; Khan, S. A. Macromolecules 2002, 35, 1699.
12. Yang, C. C.; Huang, S. H. Food Sci (Taipei) 1990, 17, 260.
13. Lai, L. S.; Chao, S. J. J Food Sci 2000, 65, 954.
14. Stossel, T. P. Science 1993, 260, 1086.
15. Sato, M.; Schwarz, W. H.; Pollard, T. D. Nature 1987, 325, 828.
16. Janmey, P. A.; Hvidt, S.; Lamb, J.; Stossel, T. P. Nature 1990, 345, 89.
17. Morris, V. J. In Gums and Stabilisers for the Food Industry 3; Philips, G. O., Wedlock, D. J., Williams, P. A., Eds.; Elsevier: London, 1985.
18. Stockmayer, W. H. J Polym Sci 1952, 9, 69.
19. Stockmayer, W. H. J Chem Phys 1943, 11, 45.
20. Tanaka, F.; Ishida, M. Macromolecules 1999, 32, 1271.
21. Flory, P. J. Principles of Polymer Chemistry; Cornell University Press: Ithaca, 1953.
22. Tanaka, F. J Polym Sci Part B: Polym Phys 2003, 41, 2413.
23. Dobson, G. R.; Gordon, M. J Chem Phys 1965, 43, 705.
24. Scanlan, J. J Polym Sci 1960, 43, 397.
25. Case, L. C. J Polym Sci 1960, 45, 501.
26. Marquardt, D. W. J Soc Ind Appl Math 1963, 11, 431.
27. Goycoolea, F. M.; Richardson, R. K.; Morris, E. R.; Gidley, M. J. Macromolecules 1995, 28, 8308.
28. Dea, I. C. M.; Morrison, A. Adv Carbohydr Chem Biochem 1975, 31, 241.
29. Dea, I. C. M.; Clark, A. H.; McCleary, B. V. Carbohydr Res 1986, 147, 275.
30. McCleary, B. V.; Clark, A. H.; Dea, I. C. M.; Rees, D. A. Carbohydr Res 1985, 139, 237.
31. Kato, K.; Matsuda, K. Agric Biol Chem Tokyo 1969, 33, 1446.
32. Nishinari, K.; Williams, P. A.; Phillips, G. O. Food Hydrocolloids 1992, 6, 199.
33. Whitney, S. E. C.; Brigham, J. E.; Darke, A. H.; Reid, J. S. G.; Gidley, M. J Carbohydr Res 1998, 307, 299.
34. Flory, P. J. J Am Chem Soc 1941, 63, 3083.
35. Blakeney, A. B.; Harris, P. J.; Henry, R. J.; Stone, B. A. Carbohydr Res 1983, 113, 291.
36. Gaisford, S. E.; Harding, S. E.; Mitchell, J. R.; Bradley, T. D. Carbohydr Polym 1986, 6, 423.
37. Torres, L. G.; Brito, E.; Galindo, E.; Choplin, L. J Ferment Bioeng 1993, 75, 58.
38. Hong, P. D.; Chen, J. H. Polymer 1998, 39, 711.
39. Morris, V. J.; Franklin, D.; I'Anson, K. Carbohydr Res 1983, 121, 13.